Molecular Investigations of Selected Spike Protein Mutations in SARS-CoV-2: Delta and Omicron Variants and Omicron Sub Variants

Urmi Roy[*]

[*]Department of Chemistry & Biomolecular Science

Clarkson University

8 Clarkson Avenue, Potsdam, NY 13699-5820, United States

[*]To whom correspondence should be addressed. E-mail: urmi@clarkson.edu; Phone: 315/212-7346; ORCID iD: https://orcid.org/0000-0003-0928-0574

Abstract:

Among the multiple SARS-CoV-2 variants recently reported, the delta variant has generated most perilous and widespread effects. Another variant, omicron, has been identified specifically for its high transmissibility. Omicron contains numerous spike (S) protein mutations and in numbers much larger than those of its predecessor variants. BA.2, a sub variant of omicron, has recently emerged with more spreadable infectivity as compared to the original omicron species. BA.2 also contains several new and additional mutations in its spike protein.

In this report we discuss some essential structural aspects and time-based structure changes of a selected set of spike protein mutations within the delta and omicron variants, including those of omicron BA.2. The expected impact of multiple-point mutations within the spike protein's receptor-binding domain (RBD) and S1 of these variants and sub variant are examined. Additionally, the more recently emerged sub variants BA.4, BA.5 and BA.2.12.1 are discussed. Within the latter group, BA.5 represents globally, the most prevalent form of SARS-CoV-2 at the present time. Time-based mutations for the sub variants BA.3 and BA.2.75 are briefly explored. It is expected that the structural data discussed in this report will be helpful to identify drug targets and to neutralize antibodies for the evolving variants/sub variants of SARS-CoV-2.

Keywords: SARS-CoV-2; spike protein; structural biochemistry; omicron sub variants; virus structure

1. Introduction

Since WHO declared a Public Health Emergency due to SARS-Cov-2 in January 2020 [1], several different variants of corona virus has emerged. Among these variants, the delta strain has been reported to be particularly aggressive due to its fast transmissibility and strong infectivity. The delta variant, also known as the B.1.617.2 strain, was first identified in India, and was listed among the CDC's "Variants of Concern" [2]. The highly contagious B.1.1.529 strain, omicron, was first identified in South Africa in December 2021 [3], and the presence of numerous spike (S) protein mutations in omicron makes this variant extremely contagious and highly transmissible. The BA.2 sub variant of omicron, containing many additional mutations in its S protein has been a predominant COVID 19 species for several months until recently [4]. At this present time, another sub variant BA.5 largely represents the most active form of coronavirus worldwide. Among the other recent omicron sub variants, BA.4 and BA.2.12.1 are also notable [5,6]. The mutations within the recent SARS-COV-2 variants and sub variants are listed in Supplementary Information (SI) Table SI 1 and SI 2.

As new variants/sub variants of SARS-CoV-2 continue to emerge, they are likely to be associated with more epitope escape mutations with unknown mutations of greater epidemiological fitness. High performance computational tools have the potential of aiding the ongoing efforts to identify the proper therapeutic targets for these pathogenic variants. In this regard, structure-based computational immunology and bioinformatics based methods of immuno-engineering play a critical role in detecting proper drug targets as well as in designing new vaccines [7-9].

In our previous reports we have discussed time-based structures of various immunologically significant proteins and their structure-functions relationships [10-12]. We have

also reported the impacts of mutations on the receptor binding domain (RBD) of SARS-CoV-2 [13,14]. Recently we have also examined the impact of Zn ion coordinated Angiotensin II peptides on the spike 1 (S1)-angiotensin converting enzyme-2 (ACE2) receptor binding [15]. In the present communication, we will analyze most of the RBD mutations observed in delta and omicron variants and omicron sub variant BA.2, and we will also determine their structural changes and stability as functions of time. Results for the time based structures of wt SARS-CoV-2 S1 and the S1 mutations within the delta, omicron, and BA.2 will be included. In addition to the above variants and sub variant, the structural changes of RBD mutations within the omicron sub variants BA.4, BA.5 and BA2.12.1 will also be discussed. Sub variants BA.4 and BA.5 contain identical RBD mutations, the details of which are included in SI tables SI 1 and SI 2 [5].

Initially we have started to explore a possible combination of delta and omicron variants and very recently a few cases of deltacron recombinant species is identified in some countries [16]. The RBD and S1 mutations within the mu and delta-omicron variants are also briefly explored here as well. Within the delta variant residue 681 is mutated to P681R. However in omicron variant this is P681H. We have kept P681R in the S1 of combined delta-omicron variant. Another variant, mu was briefly discussed in this report that was described as “Variants Being Monitored” by CDC [2]. Two other relatively new sub variants, BA.3 and BA.2.75, are also included in the SI section. The mutational details of all these sub variants are presented in SI Table SI 2 [5].

2. Materials and Methods

The spike (S) protein of the SARS CoV-2 comprised of two subunits, S1 and S2. This paper is centered on the wt and recent mutant variants of the RBD and S1 subunit. The 6M0J.PDB was selected for the wt RBD simulations [17]. Starting from the wt RBD structure, the mutant variants were generated using the VMD mutator plugin graphical user window (GUI). We have analyzed the selected S1 RBD mutations within the B.1.617.2 strain, the delta variant and the B.1.1.529 strain, the omicron variant, along with an exploration of the RBD BA.2. Among the more recently identified strains, sub variants BA.4. BA5 and BA.2.12.1 have been examined in terms of their RBD characteristics. The B.1.621 strain, also known as the mu variant and another possible combination of the delta and omicron variants has been briefly described. The structural analyses of these last two species were described in the SI. RBDs of other two sub variants BA.3 and BA.2.75 have been briefly discussed in the SI.

The I Tasser server was used to model the structure of SARS-CoV-2 S1 [18]. The wt S1 was prepared based on the 6VYB.PDB; chain B [19]. Due to the lack of experimental data, part of the protein sequences have still been missing in the published literature, making those sequences difficult to model; some of these missing sequences have been based here on the PDB structure 6ZP2 and other resources reported elsewhere [4,20]. The selected RBD and S1 mutations used in these simulation experiments have been listed in Table SI.1 and 2, and some of the mutations have been updated further through the course of this study.

For the simulation purpose we have used the NAMD, VMD and quikMD packages [21-23]. The implicit solvation system was used with the Generalized Born Solvent-Accessible Surface Area [24]. After initial minimization, annealing and equilibration processes of the MD production run were procured using the NVT ensemble. The production run was set for 25 and

20 ns for the RBD and S1 respectively. The detailed experimental procedures have been described elsewhere [13]. The resulting data were analyzed using VMD and the figures for reporting were developed using Biovia Discovery Studio Visualizer [25]. The plots of processed data were generated using origin.

3. Results and Discussions

The RBD of 6M0J.PDB contains residues 333 to 526 AAs. The RBD mutations on 6M0J are displayed in Fig.1 A-E. Fig. 1A includes the 3 mutations within the delta/ B.1.617.2 strain selected for this study. Fig. 1B includes the 15 selected mutations within the omicron/B.1.1.529 strain. Fig. 1C displays the 18 selected mutations within the omicron BA.2 sub variant. Fig.1D and 1E represents the RBD mutations within the BA.4 or BA.5 and BA. 212.1. Fig.1F-G depicts the S1 mutations in delta, omicron variants and omicron sub variant BA.2. Table SI 1 and SI 2 list the descriptive features of these mutations.

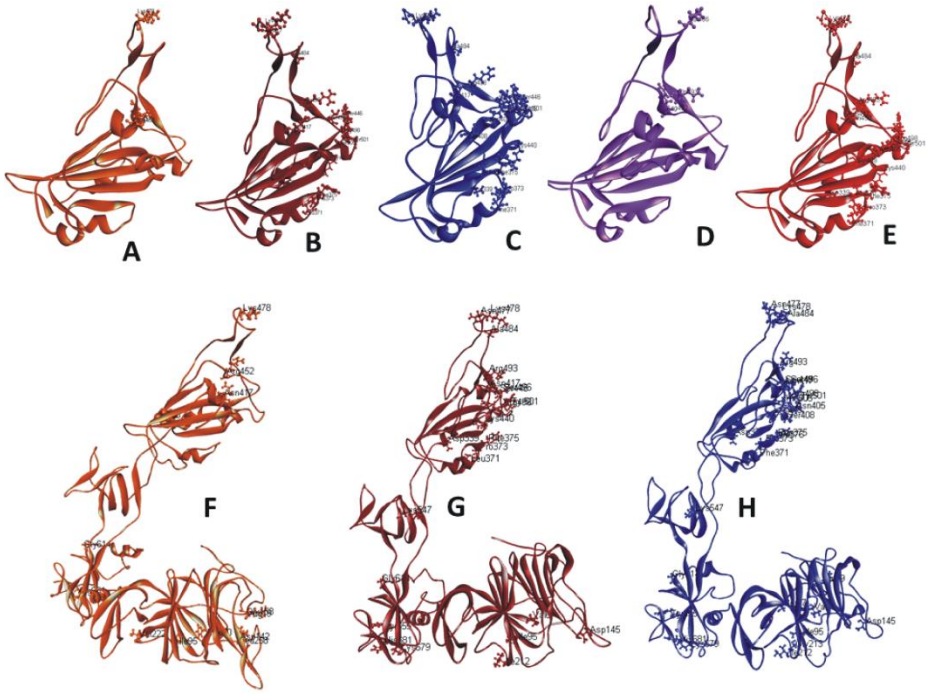

Figure 1. A-E Ribbon diagram of SARS-CoV-2 variants and sub variants with selected RBD mutations. These variants are based on 6M0J structure. Displayed are the A. delta variant with selected RBD mutations B. omicron variant with selected RBD mutations and C. Omicron BA.2 sub variant with selected RBD mutations. D. Omicron BA.4/BA.5 sub variant with selected RBD mutations. E. Omicron BA.2.12.1 sub variant with selected RBD mutations. F-H. Ribbon diagram of SARS-CoV-2 variants and sub variant with selected S1 mutations. The mutant variants and BA.2 sub variant proteins are based on S1 model structure. F. The delta variant with selected S1 mutations. G. The omicron variant with selected S1 mutations. H. The omicron sub variant BA.2 with selected S1 mutations.

The RBD mutations within sub variants BA.3 and BA.2.75, as well as the mutations in mu/B.1.621, along with a potential combined strain of delta-omicron, are tabulated there. This delta-omicron contains one additional mutation L452R from the delta variant in addition to the omicron RBD mutations. The RBD mutations of other variants have been described in our previous report [14].

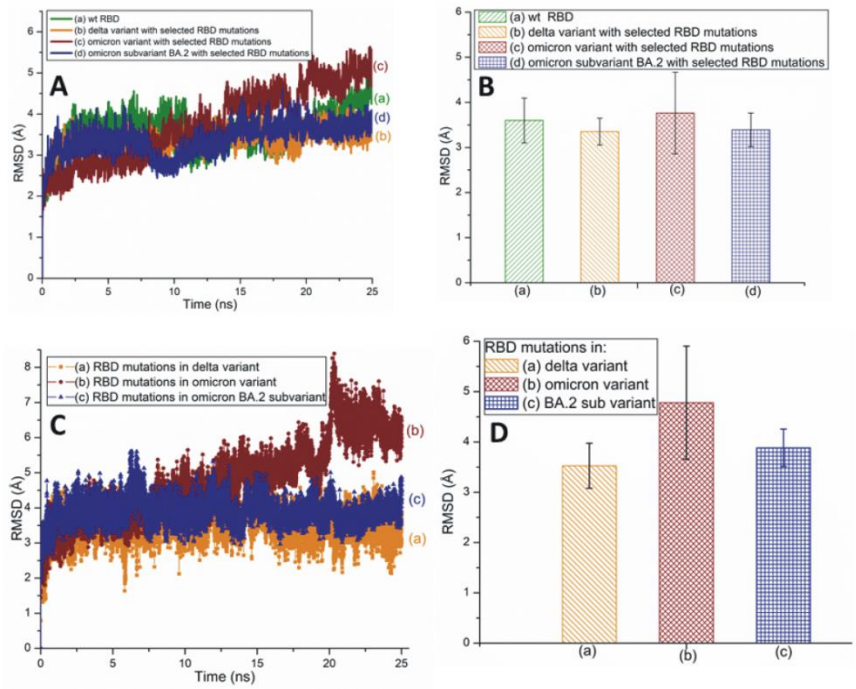

Figure 2. A. The typical RMSD plots of wt and different SARS-CoV-2 variants and sub variant with selected RBD mutations. These variants and sub variant are based on 6M0J structure. B The average RMSD plot of wt RBD, delta, omicron and BA.2 sub variant with selected RBD mutations. These values are extracted from Fig. 2A. The average RMSD value was taken from a 25ns simulation time. C. The typical RMSD plots of RBD mutations within different SARS-CoV-2 variants and sub variant. D. The average RMSD plots for SARS-CoV-2 mutations within deferent variants. The average values are extracted from Fig. 2C.

Fig. 2A illustrates the traditional RMSD plots of wt and different SARS-CoV-2 variants with selected RBD mutations; wt SARS-CoV-2 has also been included here for comparison. It is evident from this plot that delta RBD is the most stable form among all species studied here. This variant is more stable than omicron and even stable compare to its wt version. While the omicron variant is most unstable, the RBD of omicron sub variant BA.2 is quite stable. The average root mean square deviation (RMSD) of the BA.2 sub variant is slightly higher than that of the delta variant as displayed in Fig. 2B. Fig. 2B also describes the RMSD results within the delta and omicron species. The delta variant has the lowest average RMSD values while omicron has the highest. This figure also indicates certain findings from Fig. 2A, where the omicron variant shows larger variations. Fig. 2C presents the RMSD plots of RBD mutations within different variants. The results in Figs 2C-2D suggest that the mutations in the delta variant are most stable and those of omicron are most unstable. It is possible that numerous RBD mutations within the omicron make the latter unstable; this is not the case for the RBD of omicron sub variant BA.2, where the presence of RBD mutations make this protein rather stable.

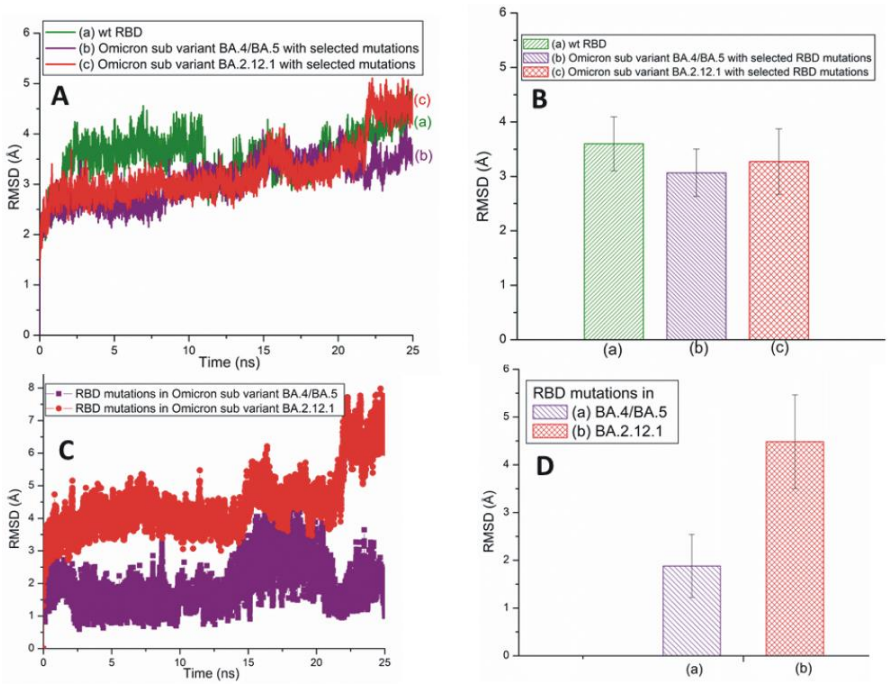

Figure 3. A. The typical RMSD plots of wt and recently emerged SARS-CoV-2 omicron sub variants with selected RBD mutations. These sub variants are based on 6M0J structure. B The average RMSD plot of wt RBD, sub variants BA.4/BA.5 and BA.2.12.1 with selected RBD mutations. The values were taken from the 25 ns simulation time. These values were extracted from Fig. 3A. C. The typical RMSD plots of RBD mutations within recently emerged SARS-CoV-2 sub variants BA.4/BA.5 and BA.2.12.1. D. The average RMSD plots for SARS-CoV-2 mutations within deferent sub variants. The average values are extracted from Fig. 3C.

Fig. 3A illustrates traditional RMSD plots of the SARS-CoV-2 omicron sub variants, BA.4/BA.5 and BA.2.12.1 with selected RBD mutations. The average RMSD values of these sub variants are displayed in Fig. 3B. From Fig.3A-B it is evident that RBD of sub variant BA.4/BA.5 is more stable than both the wt and the BA.2.12.1 RBDs. The RMSD of RBD mutations within these two sub variants are plotted in Fig. 3C-3D, and these plots mimic Figs.3A and B. The mutations within BA.4/BA.5 are also more stable than those existing within BA.2.12.1. Overall, the RBD mutations within BA.4/BA.5 are more stable than those of delta and omicron variants, as well as BA.2 and BA.2.12.1 sub variants (Fig 2C and D).

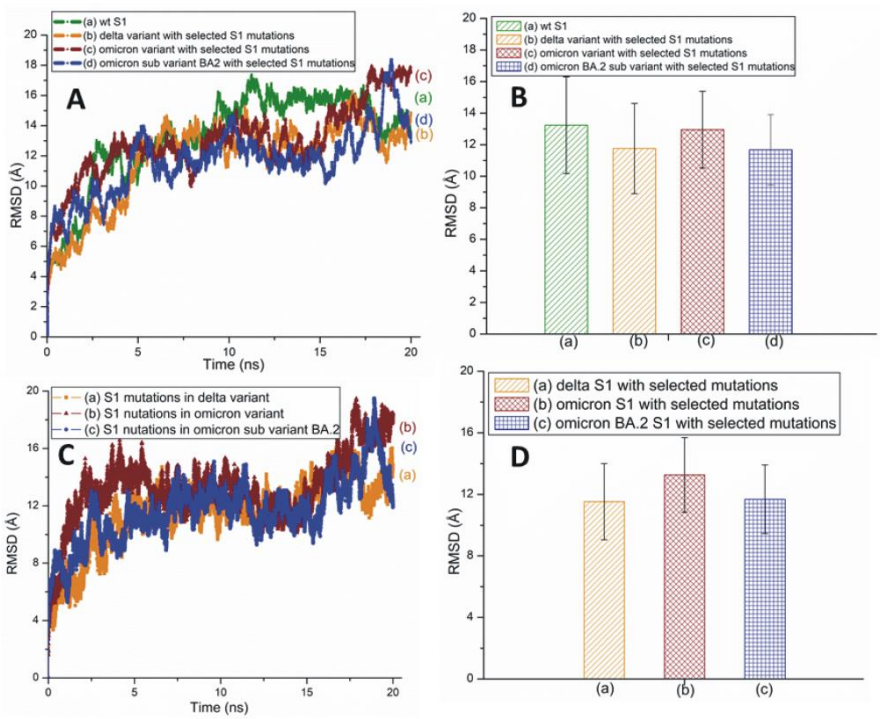

Figure 4. A. The typical RMSD plots of wt and different SARS-CoV-2 variants and sub variant with selected S1 mutations. These variants and sub variant are based on model SARS-CoV-2 S1structure. B The average RMSD plot of wt S1, the delta and omicron variants and omicron sub variant BA.2 with selected S1 mutations. The average RMSD value was taken from a 20ns simulation time. These values were extracted from Fig. 4A. C. The typical RMSD plots of S1 mutations within different SARS-CoV-2 variants and sub variant. D. The average RMSD plots for SARS-CoV-2 mutations within deferent variants. The average values were extracted from Fig. 4C.

Fig. 4A represents the traditional RMSD graphs of the wt and the mutant variants of SARS-CoV-2 S1 with selected mutations. Fig 4B shows the average RMSD values of the wt and variant proteins with selected S1 mutations. From these plots we can infer that the omicron variant and BA.2 sub variant with S1 mutations show higher RMSD values compare to those of the delta variant. It is also clear from Fig. 4C-D that the S1 mutations within the delta variant show the lowest degree of RMSD variations. Therefore, we can assume that delta variant is the most stable form of this virus among these variants and sub variant. Interestingly, at the same time, the S1 of BA.2 shows marginally lower RMSD (11.67Å) than delta S1 (11.76Å) though the RBD of delta (3.35Å) seems slightly more stable than the BA.2 RBD (3.39Å). The overall RMSD values of the S1 are much higher than the RBD RMSDs due to the presence of many turns and coils in this segment.

Results of time based secondary structure analyses of different RBDs are displayed in Fig. 5. Within the delta variant, the secondary structure of K417N and L452R mutations are stable compared to T478K (Fig. 5A). In the omicron variant most of the mutations are unstable including G339D, S371L, S375F, N440K, S477N and T478K, which, in combination, make the omicron RBD measurably unstable (Fig. 5B). In BA.2 sub variant R408S, T478K and E484A residues seems very stable whereas residues G339D and G496S appear unstable (Fig.5C). These results, suggest an overall high stability of the delta RBD. Based on its RBD, the sub variant

BA.2 is also a stable protein and omicron RBD is most unstable among these three RBDs. All the three mutations identified in BA.4/BA.5, displayed in Fig.5D, are quite stable. Fig. 5E represents the secondary structure changes of the RBD mutations within BA.2.12.1 sub variant. While mutation R408S appears stable with time, according to the present results, mutations S371F, K417N and T478K do not seem to follow the same the same trend.

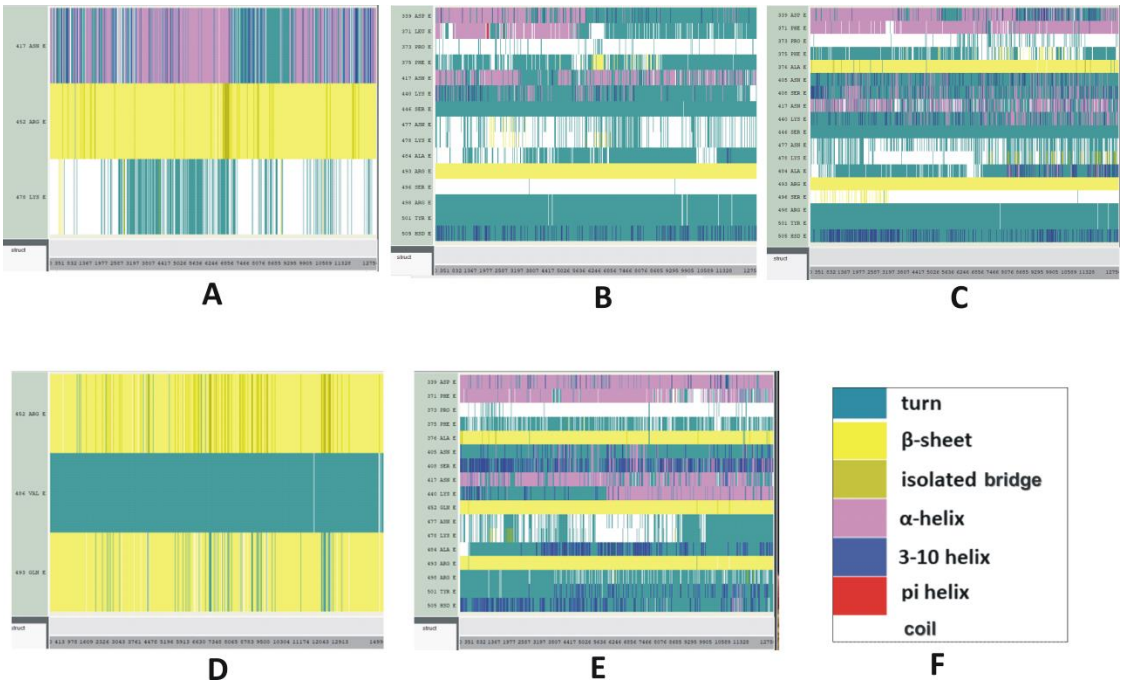

Figure 5. Time based secondary structure changes of SARS-CoV-2 mutant variants and sub variants. The vertical axis represents the mutated residues and the horizontal axis represents the simulation trajectory. A-E. the SARS-CoV-2 RBD of (A) delta, (B) omicron variants and omicron sub variants (C) BA.2 (D) BA.4/BA.5 (E) BA.2.12.1 with selected RBD mutations. These secondary structural changes were recorded for 25ns. F. Color code explanation of proteins' secondary structures. These are the default color codes generated by VMD GUI.

Fig. 6 illustrates the secondary structure changes of SARS-CoV-2 S1 of delta, and omicron variants and BA.2 sub variant with selected S1 mutations. The delta S1 appears quite stable (Fig.6A). No major changes in the stability or fluctuations within the secondary structures are observed for this variant. V70F and T478K residues also seem quite stable during the simulation timescale as the turns and coils of these species are converted into beta sheets. In the

case of omicron S1, though residues G339D and N440K seem stable with time, fluctuations are observed in the mutated residues A67V, L212I, K417N and T547K (Fig. 6B). For the BA.2 sub variant (Fig.6C), residues V47 and T478K seem unstable as their beta sheets are converted into turns and coils. On the other hand, residues F375, 479-81 are converted to alpha helices and beta sheets from their turns/coils phases, respectively. The stability analyses of S1 secondary structure mimics those of the RBD secondary structures, and suggests that delta is the most stable variant, while the BA.2 sub variant is more stable than omicron.

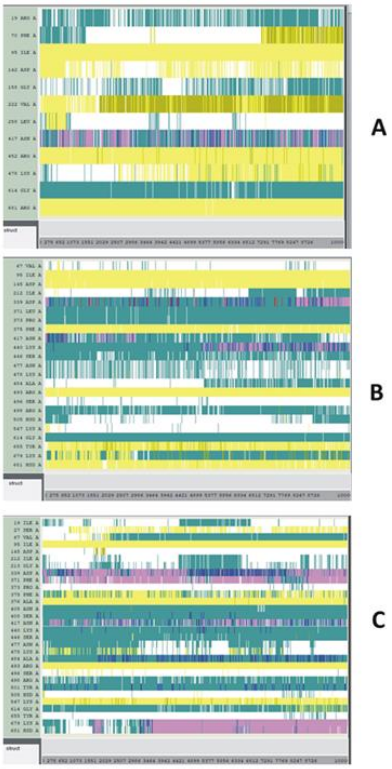

Figure 6. The Secondary structure changes of SARS-CoV-2 S1 . A. delta and B. omicron variants and C. omicron sub variant BA.2 with selected S1 mutations. The structural changes were recorded for 20ns.

The average solvent accessible surface area (SASA) values for each of the RBD and S1 mutations within the SARS-CoV-2 variants and sub variants are plotted in Fig.7. These results are average SASA values obtained from the simulation time scale. The SASA values are calculated using the VMD timeline window. It should be noted in this context that the severity of certain disease largely depends on the buried or exposed nature of the underlying mutated

residues [26]. In Fig. 7A, the highest SASA values are observed in L452R within the RBD of delta variant, which suggests that this residue has a comparably large solvent accessible surface. The SASA values may increase due to partial unfolding caused by residue mutation.

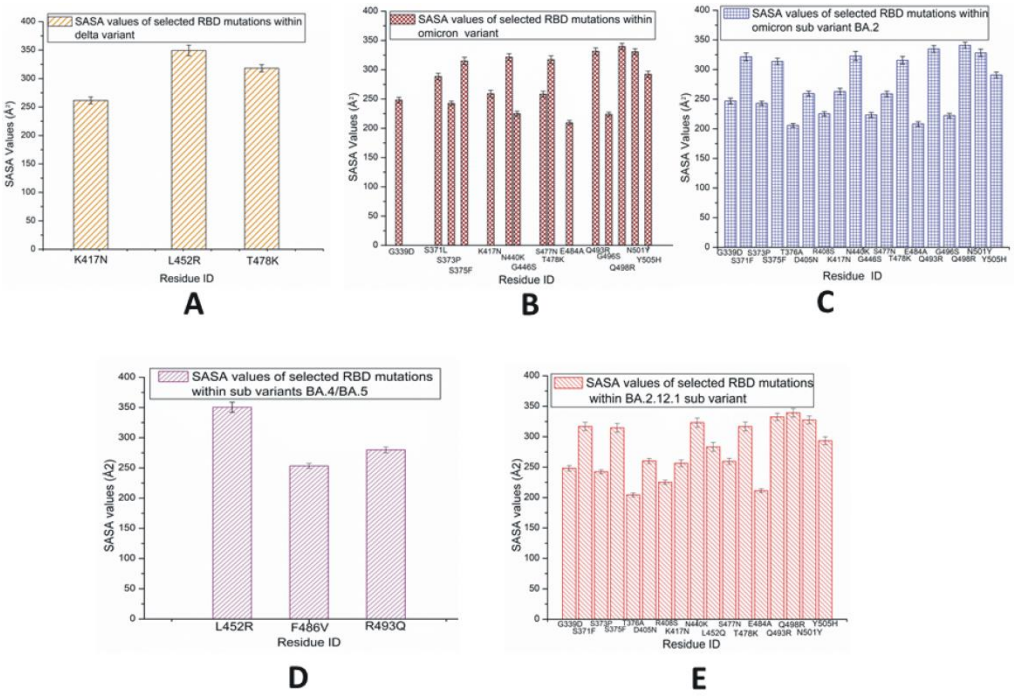

Figure 7. Average SASA values of SARS-CoV-2 RBD mutations observed predominantly in variants A. delta; B. omicron and sub variants C. BA.2; D. BA.4/BA.5; and E. BA.2.12.1.

Among the three species we have studied here, the L452R mutation is only observed in the delta variant. Since mutated residue R is hydrophilic and surface exposed, the structural rearrangements or conformational deviations may possible in this case. Published report suggests that L452R within the delta variant strongly interacts with ACE2 [27]. T478K within delta variant also shows considerably high SASA value. As positively charged K^+ impact the electrostatic surface area, this residue may manifest stronger interactions with the receptor [28]. In delta RBD, only one residue shows considerably lower SASA values indicating that this buried residue K417N is quite stable in nature. However, if surface exposed residues on the RBD form stable interactions with the ACE2 receptor as in the case of delta, where the mutant L452R

strongly bind to the ACE2 receptor making delta RBD quite stable. Thus it could be possible that the L452R and T478K within the delta variant may have a stronger stabilizing effect [14,29]. Although T478K was not present in any previously identified variants, this mutation is observed in all the variants and sub variant we studied in this report. It is possible that the greater mutational fitness of the delta variant may be due to L452R or a combination of a number of residue mutations.

In the case of omicron RBD, as displayed in Fig. 7B, despite the presence of fewer buried residues with lower SASA values, majority of the mutated residues have greater SASA values; this suggests the possibility of making this protein quite unstable as S protein of omicron variant demonstrated decreased receptor interactions [30].

The omicron variant contains more mutations than delta and some of them are at the ligand-receptor interfacial region, while the stronger binding interactions between L452R and ACE2 receptor make delta variant somewhat unique. Hydrogen bond formation between residue G493 of delta with ACE2 contributes to it stronger structure [27]. Furthermore, it is possible that most of the mutations present in the omicron variant are counteracted by neutralizing antibodies, while at the same time, L452R in delta is considered as antibody neutralizing escape mutation.

In the case of BA.2, as displayed in Fig.7C the slightly higher numbers of buried residues (with lower SASA values) possibly make this sub variant more stable than original omicron. Usually, the buried residues present within the core of the protein are the most stable part of a protein. The surface exposed residues with greater SASA values are likely to be comparatively less stable unless the surface exposed residues form stronger receptor interactions.

Fig. 7D represents the SASA values of RBD mutations within BA.4/BA.5. Here mutation L452R demonstrates higher SASA values compared to those of the other two mutations, F486V

and R493Q. Among the other strains studied in this report, mutation L452R is only present in the delta variant. In BA.2.12.1, the 452 mutation is denoted as L452Q. It is possible that the BA.5 sub variant has become a dominant strain due to the antibody neutralization escape nature of L452R.Considering that the RBDs of BA.4 and BA5 contain mutually similar mutations, certain structural/mutational differences within the S protein may exist that make BA.5 more transmissive than BA.4. The SASA values of RBD mutations in BA.2.12.1 are displayed in Fig. 7E. Although some relatively low SASA values are observed, majority of the BA.2.12.1 mutations are surface exposed and contain greater SASA values. Overall, BA.2 sub variant has more buried residues than those of BA.212.1.

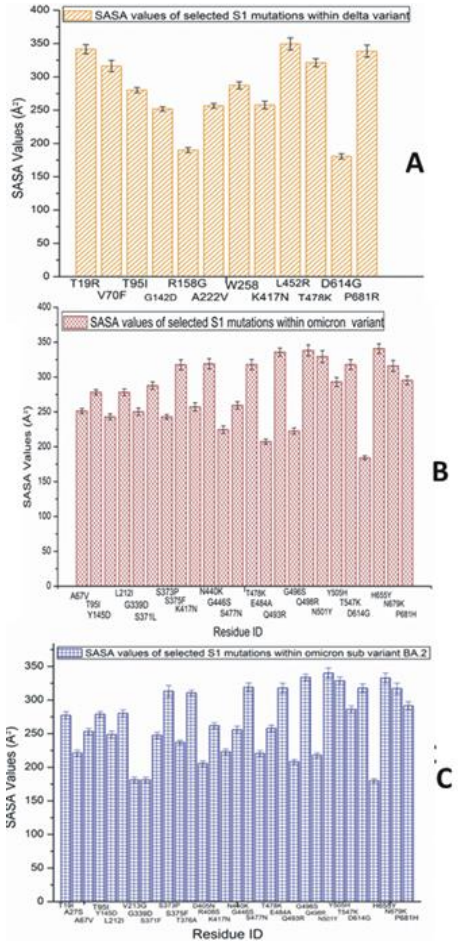

Figure 8. Average SASA values of SARS-CoV-2 S1 mutations observed predominantly in A. delta variant; B. omicron variant; and C. omicron sub variant BA.2.

The SASA values of S1 mutations are displayed in Fig 8A-C, where the findings of the corresponding RBDs are detected again. The delta has a number of buried residues, but here the surface exposed residues have strong interactions with ACE2. Despite the many buried residues of omicron, the numbers of surface exposed residues are greater than the buried residues in this case. S1 of sub variant BA.2 has more buried residues than those of the S1 of omicron variant. It is likely that most of the surface exposed residues in the omicron variant are loosely attached to the ACE2 receptor. Currently there are no readily available experimental results for the BA.2 sub variant. It could be possible that the surface exposed residues within sub variant BA.2 bind more strongly to the ACE2 receptor than omicron variant. This sub variant may have antibody neutralizing escape mutants and thus, may emerge as a strong form of the virus [31,32]. Nonetheless, according to the RMSD data and the time-based secondary structure analyses of S1 data presented here, the delta is currently most stable, sub variant BA.2 also is quite stable among the three forms we have studied. The delta-omicron species also shows low RMSD values (Fig. SI. 3). For the RBD structure, BA.4/BA. 5 is the most stable form along with delta variant and BA.2 sub variant. Since most of the mutations in BA.4, BA.5 and BA2.12.1 are concentrated and hence observed in their RBDs, we have specifically examined the RBDs of these three sub variants in the present report.

4. Conclusions

The simulation data reported here indicate that delta is a stable form of COVID 19 and the omicron BA.2 sub variant is also quite stable. However, among the forms selected for the present study, BA.4/BA.5 RBD appears most stable. We expect that the structural data discussed in this paper will be useful to identify drug targets and neutralizing antibodies for emerging

SARS-CoV-2 variants or sub variants with newer escape mutations. We also hope that by contributing to the literature on SARS-CoV-2, the present manuscript will serve to help the ongoing efforts to overcome the COVID 19 pandemic in some ways.

Omicron sub variant BA.2 has been known as "stealth omicron" as this sub variant was initially difficult to identify from the delta variant using traditional testing procedures. Recently, a combination of sub variants BA.1 and BA.2 has been reported. This hybrid or recombinant variant is also known as sub variant XE [33]. As the mRNA virus is highly adaptable and environmentally fit, it is possible that newer sub versions of variants/sub variants would arise with new functional epitopes and with new escape mutations.

Supplemental Information

Figs SI 1-6; Table SI 1-2

Conflict of interest statement

The author declares no conflict of interest.

Acknowledgments

The author acknowledges utilization of the following simulation and visualization software packages: 1) NAMD and 2) VMD: NAMD and VMD, developed by the Theoretical and Computational Biophysics Group in the Beckman Institute for Advanced Science and Technology at the University of Illinois, Urbana-Champaign. 3) Discovery Studio Visualizer: Dassault Systèmes BIOVIA, Discovery Studio Modeling Environment, San Diego, CA: Dassault Systèmes (2015).

References

1. WHO, Weekly epidemiological update (2021). Available online: https://www.who.int/publications/m/item/weekly-epidemiological-update---23-february-2021 (accessed on 25 February 2021).
2. https://www.cdc.gov/coronavirus/2019-ncov/variants/variant-info.html#Interest. Centers for Disease Control and Prevention, SARS-CoV-2 Variant Classifications and Definitions. Available online: https://www.cdc.gov/coronavirus/2019-ncov/variants/variant-info.html#Interest. (accessed on June 22, 2021, July 26, 2021, December7, 2021, April 26, 2022).
3. https://www.cdc.gov/coronavirus/2019-ncov/science/science-briefs/scientific-brief-omicron-variant.html. Science Brief: Omicron (B.1.1.529) Variant. Available online: https://www.cdc.gov/coronavirus/2019-ncov/science/science-briefs/scientific-brief-omicron-variant.html (accessed on February 18, 2022).
4. https://covariants.org/variants/21L.Omicron. Variant: 21L (Omicron) also known as BA.2. Available online: https://covariants.org/variants/21L.Omicron (accessed on March 22, 2022).
5. SARS-CoV-2 variants of concern as of 9 June 2022. Available online: https://www.ecdc.europa.eu/en/covid-19/variants-concern (accessed on June 17, 2022, July 12, 2022).
6. Tracking SARS-CoV-2 variants. Available online: https://www.who.int/en/activities/tracking-SARS-CoV-2-variants/ (accessed on June 14, 2022).
7. Lampe, A.T.; Puniya, B.L.; Pannier, A.K.; Helikar, T.; Brown, D.M. Combined TLR4 and TLR9 agonists induce distinct phenotypic changes in innate immunity in vitro and in vivo. *Cell. Immunol.* **2020**, *355*, 104149.
8. Haspel, N.; Jang, H.; Nussinov, R. Active and Inactive Cdc42 Differ in Their Insert Region Conformational Dynamics. *Biophys. J.* **2021**, *120*, 306-318.
9. Schneidman-Duhovny, D.; Wolfson, H.J. Modeling of Multimolecular Complexes. *Methods Mol. Biol.* **2020**, *2112*, 163-174.
10. Roy, U. Structural Characterizations of the Fas Receptor and the Fas-Associated Protein with Death Domain Interactions. *The Protein J.* **2016**, *35*, 51-60.
11. Roy, U. 3D Modeling of Tumor Necrosis Factor Receptor and Tumor Necrosis Factor-bound Receptor Systems. *Mol. Inform.* **2019**, *38*, e1800011.
12. Roy, U. Structural and molecular analyses of functional epitopes and escape mutants in Japanese encephalitis virus envelope protein domain III. *Immunol. Res.* **2020**, *68*, 81-89.
13. Roy, U. Role of N501Y mutation in SARS-CoV-2 spike proteinstructure. *Preprints, 2021060238* **2021**.
14. Roy, U. Comparative Structural Analyses of Selected Spike Protein-RBD Mutations in SARS-CoV-2 Lineages. *Immunol. Res.* **2021**, *70*, 143-151.
15. Fatouros, P.R.; Roy, U.; Sur, S. Modeling Substrate Coordination to Zn-Bound Angiotensin Converting Enzyme 2. *Int. J. Pept. Res. Ther.* **2022**, *28*, 65.
16. https://www.cnbc.com/2022/01/08/cyprus-reportedly-discovers-a-covid-variant-that-combines-omicron-and-delta.html. Cyprus reportedly discovers a Covid variant that combines omicron and delta. Health and Science Available online: https://www.cnbc.com/2022/01/08/cyprus-reportedly-discovers-a-covid-variant-that-combines-omicron-and-delta.html (accessed on accessed January 2022).
17. Huo, J.; Zhao, Y.; Ren, J.; Zhou, D.; Duyvesteyn, H.M.E.; Ginn, H.M.; Carrique, L.; Malinauskas, T.; Ruza, R.R.; Shah, P.N.M.; et al. Neutralization of SARS-CoV-2 by Destruction of the Prefusion Spike. *Cell Host Microbe* **2020**, *28*, 445-454.e446.

18. Yang, J.; Zhang, Y. I-TASSER server: new development for protein structure and function predictions. *Nucleic Acids Res.* **2015**, *43*, W174-181.
19. Walls, A.C.; Park, Y.J.; Tortorici, M.A.; Wall, A.; McGuire, A.T.; Veesler, D. Structure, Function, and Antigenicity of the SARS-CoV-2 Spike Glycoprotein. *Cell* **2020**, *181*, 281-292.e286.
20. Xiong, X.; Qu, K.; Ciazynska, K.A.; Hosmillo, M.; Carter, A.P.; Ebrahimi, S.; Ke, Z.; Scheres, S.H.W.; Bergamaschi, L.; Grice, G.L.; et al. A thermostable, closed SARS-CoV-2 spike protein trimer. *Nat. Struct. Mol. Biol.* **2020**, *27*, 934-941.
21. Humphrey, W.; Dalke, A.; Schulten, K. VMD: Visual molecular dynamics. *J. Mol. Graph.* **1996**, *14*, 33-38.
22. Phillips, J.C.; Braun, R.; Wang, W.; Gumbart, J.; Tajkhorshid, E.; Villa, E.; Chipot, C.; Skeel, R.D.; Kale, L.; Schulten, K. Scalable molecular dynamics with NAMD. *J. Comput. Chem* **2005**, *26*, 1781-1802.
23. Ribeiro, J.V.; Bernardi, R.C.; Rudack, T.; Stone, J.E.; Phillips, J.C.; Freddolino, P.L.; Schulten, K. QwikMD - Integrative Molecular Dynamics Toolkit for Novices and Experts. *Sci. Rep.* **2016**, *6*, 26536.
24. Tanner, D.E.; Phillips, J.C.; Schulten, K. GPU/CPU Algorithm for Generalized Born/Solvent-Accessible Surface Area Implicit Solvent Calculations. *J. Chem. Theory Comput.* **2012**, *8*, 2521-2530.
25. Dassault Systèmes BIOVIA *Discovery Studio Modeling Environment, San Diego, CA: Dassault Systèmes (2015).*
26. Savojardo, C.; Manfredi, M.; Martelli, P.L.; Casadio, R. Solvent Accessibility of Residues Undergoing Pathogenic Variations in Humans: From Protein Structures to Protein Sequences. *Front Mol. Biosci.* **2020**, *7*, 626363.
27. Socher, E.; Heger, L.; Paulsen, F.; Zunke, F.; Arnold, P. Molecular dynamics simulations of the delta and omicron SARS-CoV-2 spike - ACE2 complexes reveal distinct changes between both variants. *Comput. Struct. Biotechnol. J.* **2022**, *20*, 1168-1176.
28. Di Giacomo, S.; Mercatelli, D.; Rakhimov, A.; Giorgi, F.M. Preliminary report on severe acute respiratory syndrome coronavirus 2 (SARS-CoV-2) Spike mutation T478K. *J. Med. Virol.* **2021**, *93*, 5638-5643.
29. Goher, S.S.; Ali, F.; Amin, M. The Delta Variant Mutations in the Receptor Binding Domain of SARS-CoV-2 Show Enhanced Electrostatic Interactions with the ACE2. *Med. Drug Discov.* **2021**, 100114.
30. Zeng, C.; Evans, J.P.; Qu, P.; Faraone, J.; Zheng, Y.-M.; Carlin, C.; Bednash, J.S.; Zhou, T.; Lozanski, G.; Mallampalli, R.; et al. Neutralization and Stability of SARS-CoV-2 Omicron Variant. *bioRxiv* **2021**, 2021.2012.2016.472934.
31. Chen, J.; Wei, G.-W. Omicron BA.2 (B.1.1.529.2): high potential to becoming the next dominating variant. *ArXiv* **2022**, arXiv:2202.05031v05031.
32. Kannan, S.R.; Spratt, A.N.; Sharma, K.; Sönnerborg, A.; Apparsundaram, S.; Lorson, C.; Byrareddy, S.N.; Singh, K. Complex Mutation Pattern of Omicron BA. 2: Evading Antibodies without Losing Receptor Interactions. *Int. J. Mol. Sci.* **2022**, *23*, 5534.
33. https://www.foxnews.com/health/covid-19-subvariant-xe-ba-2-coronavirus-pandemic. COVID-19 subvariant XE: What to know. Available online: https://www.foxnews.com/health/covid-19-subvariant-xe-ba-2-coronavirus-pandemic (accessed on accessed May 10, 2022).